A perturbed two-level model for exciton trapping in small photosynthetic systems.

Somsen, O.J.G.; Valkunas, L.; van Grondelle, R.

published in
Biophysical Journal
1996

DOI (link to publisher)
10.1016/S0006-3495(96)79607-8

document version
Publisher's PDF, also known as Version of record

A Perturbed Two-Level Model for Exciton Trapping in Small Photosynthetic Systems

Oscar J. G. Somsen,* Leonas Valkunas,‡ and Rienk van Grondelle*
*Free University Amsterdam, Department of Physics and Astronomy, De Boelelaan 1081, 1081 HV Amsterdam, The Netherlands and ‡Institute of Physics, A. Gostauto 12, 2600 Vilnius, Lithuania

ABSTRACT The study of exciton trapping in photosynthetic systems provides significant information about migration kinetics within the light harvesting antenna (LHA) and the reaction center (RC). We discuss two random walk models for systems with weakly coupled pigments, with a focus on the application to small systems (10–40 pigments/RC). Details of the exciton transfer to and from the RC are taken into consideration, as well as migration within the LHA and quenching in the RC. The first model is obtained by adapting earlier local trap models for application to small systems. The exciton lifetime is approximated by the sum of three contributions related to migration in the LHA, trapping by the RC, and quenching within the RC. The second model is more suitable for small systems and regards the finite rate of migration within the LHA as a perturbation of the simplified model, where the LHA and the RC are each represented by a single pigment level. In this approximation, the exciton lifetime is the sum of a migration component and a single nonlinear expression for the trapping and quenching of the excitons. Numerical simulations demonstrate that both models provide accurate estimates of the exciton lifetime in the intermediate range of 20–50 sites/RC. In combination, they cover the entire range of very small to very large photosynthetic systems. Although initially intended for regular LHA lattices, the models can also be applied to less regular systems. This becomes essential as more details of the structure of these systems become available. Analysis with these models indicates that the excited state decay in LH1 is limited by the average rate at which excitons transfer to the RC from neighboring sites in the LHA. By comparing this to the average rate of transfer within the LHA, various structural models that have been proposed for the LH1 core antenna are discussed.

INTRODUCTION

Two pigment-protein complexes contribute to the process of primary photosynthesis. The reaction center (RC) absorbs sunlight and creates a charge separation with the energy. This occurs on a time scale of 1–10 ps in a variety organisms and is largely irreversible. The RC is assisted by a light harvesting antenna (LHA). This network of pigment-protein complexes contains 20–10,000 densely ($\gtrsim$ 1 pigments/nm^2) packed pigments per RC, in a variety of structural organizations. They absorb additional light and direct it to the RC (van Grondelle et al., 1994). In the presence of an LHA, excited state decay slows down to 50–100 ps, with surprisingly little dependence on the size of the antenna. Because this is short with respect to loss channels such as fluorescence ($\simeq$ 1 ns), the quantum yield of trapping is hardly affected. However, the lifetime increase can be observed and provides information about the structural organization of the LHA-RC system.

A suitable system to study the excited-state decay is the photosynthetic purple bacterium *Rhodospirillum (Rs.) rubrum*. It contains a single antenna species (LH1), which forms a well-defined core complex, the photosynthetic unit (PSU), around the RC at a fixed stoichiometry of 24 bacteriochlorophyll (Bchl) a pigments and 12 pairs of a small α- and β-polypeptide, each with a single membrane spanning helix (Cogdell et al., 1982; Aagaard and Sistrom, 1972; Stark et al., 1983; Meckenstock et al., 1992). A six-fold symmetric structure around the RC was observed with electron microscopy (Stark et al., 1983), indicating that the basic unit of the PSU is either $\alpha\beta$Bchl$_2$ or $\alpha_2\beta_2$Bchl$_4$. Single $\alpha\beta$Bchl$_2$ units, the so-called "B820" subunits, have been isolated from LH1 (Loach et al., 1985; Visschers et al., 1991). In reconstituted PSUs, a ringlike structure of 16 $\alpha\beta$Bchl$_2$ subunits was recently observed with high resolution electron microscopy (Karrasch et al., 1995). Triplet-minus-singlet spectroscopy (van Mourik et al., 1991; Visschers et al., 1991) and the similarity between the spectra of B820 and LH1 indicate that the Bchl pigments from strongly coupled dimers in a head-tail configuration. A number of PSUs are organized in larger clusters.

Exciton kinetics in the LH1 core complex

Much research has been done regarding the excited-state kinetics in the LH1 core antenna. The overall exciton lifetime is 60 ps (Freiberg et al., 1989; Timpmann et al., 1991; Pullerits et al., 1994). This is a combined result of migration in the LHA, transfer between the LHA and the RC, and the sharing of one decay channel in the RC by many pigments. These three processes have also been studied separately. The charge separation takes 3–3.5 ps in isolated RCs (Martin et al., 1986), and 4.5 ps in membranes (Schmidt et al., 1993). Its rate has not been observed in intact systems.

Received for publication 13 July 1995 and in final form 24 October 1995.
Address reprint requests to R. van Grondelle, Department of Physics and Astronomy, Free University Amsterdam, De Boelelaan 1081, Amsterdam 1081 HV, The Netherlands. Tel.: +31-20-444-7930; Fax: +31-20-444-7899.

0006-3495/96/02/669/00 $2.00

Direct information about exciton transfer within the antenna is obtained from singlet-singlet annihilation studies. This process occurs when two or more excitons are present in one domain; it does not involve the RC. It was observed by measuring the fluorescence quantum yield (Bakker et al., 1983; den Hollander et al., 1983; Trinkunas and Valkunas, 1989) or excited-state decay kinetics (Valkunas, 1989a; Valkunas et al., 1995) as a function of the excitation light intensity. From these studies, the transfer (or "hopping") time between neighboring pigments was estimated to be 0.65 ps. This fast transfer, which takes at most a few picoseconds, is confirmed by polarization decay in time-resolved absorption and fluorescence measurements (van Grondelle et al., 1987). In recent upconversion experiments, the fluorescence polarization decay time was determined to be 0.35 ps (Bradforth et al., 1995). In addition, a transient red shift of absorption difference spectra was observed on a time scale of 0.3 ps and attributed to thermal equilibration within the antenna (Visser et al., 1995).

Transfer between neighboring PSUs also takes place. This was demonstrated by observing the fluorescence quantum yield as a function of the fraction of closed RCs (Vredenberg and Duysens, 1963; Bakker et al., 1983; den Hollander et al., 1983), and by singlet-singlet (Valkunas, 1989b) and singlet-triplet annihilation studies (Monger and Parson, 1970).

Transfer between LHA and RC has been investigated by selective excitation of the RC. Time resolved experiments in *Rs. rubrum* indicate that 20–30% of the excitons "escape" to the LHA (Timpmann et al., 1993). Similar conclusions were obtained by pump-probe experiments on *Chromatium minutissimum* (Abdourakhmanov et al., 1989), *Rhodobacter capsulatus* (Xiao et al., 1994), and *Rhodopseudomonas (Rps.) viridis* (Timpmann et al., 1995). Published steady-state fluorescence excitation spectra of *Rps. viridis*, and 6 K of *Rps. viridis* and *Rs. rubrum* indicate that fluorescence is completely quenched upon selective excitation of the RC (Otte et al., 1993), but some amount of escape was observed in other excitation spectra (Visschers et al., personal communication). This difference may be due to the presence of a small fraction of PSUs without a functional RC.

Finally, the effect of the kinetics within the RC on the trapping process was investigated in site-specific RC mutants of *Rhodobacter sphaeroides* (Beekman et al., 1994) lacking LH2. The variation of the time-constant of charge separation, from 3.5 to 15 ps in these mutants, has limited effect on the exciton lifetime in the LHA, in accordance with the idea that charge separation is not the limiting step (Valkunas et al., 1992; Somsen et al., 1994).

Energy migration models

To interpret all this data within a consistent LH1 model, it is necessary to describe the relation between the model's structure and the exciton transfer kinetics. Various theories have been developed, initially to explain the fluorescence properties of concentrated dye solutions. As described by Förster, the rate of transfer between weakly interacting pigments is proportional to the spectral overlap of the fluorescence spectrum of the donor, the absorption spectrum of the acceptor, and the square of the electronic interaction between them (Förster, 1965). In the case of dipole-dipole interaction it falls off with the sixth power of the distance. This situation changes when the excitonic interaction is of the same order or stronger than the energetic disorder. In that case a set of delocalized states is formed, and transfer occurs between such states instead. In LH1 strong dimer interaction has been demonstrated and even further delocalization has been proposed (Dracheva et al., 1994).

Once the transfer between individual pigments is known, a kinetic model of the photosynthetic system can be constructed (Pullerits and Freiberg, 1992). In the simplest representation, the pigments of LHA and RC are sites on a regular lattice. Trapping is modelled by including the charge separation as an additional decay rate at the RC site. A set of differential equations describes the exciton kinetics. In view of the increasing knowledge about the composition and structure of LH1 and other antennas, deviations from this regular model may be considered. First, the large size of the RC protein with respect to the $\alpha\beta Bchl_2$ unit of LH1 implies that transfer to and from the RC is slow, but also that the RC has more neighbors than the sites within the LHA. Second, the clustering of pigments may lead to delocalization or differentiation of transfer rates, which may be aggravated by the effects of pigment orientations. Finally, the transfer rates within the PSU may differ from the rates to neighboring PSUs.

These considerations can partly be included as corrections to the regular lattice model. For example, the altered transfer to and from the RC (but not the number of neighbors) can be included as additional parameters. The strongly coupled dimer in LH1 can be represented by a single site. In principle, both excitonic states must be considered, but in the typical head-tail configuration, the blue-shifted state contains almost no dipole strength and is not populated if the excitonic splitting is larger than the Boltzmann factor. Therefore, this state can be disregarded. Similarly, larger clusters can also be treated as a single site if internal equilibration is faster than the transfer between clusters. Care should be taken when interpreting rate parameters in such a model, because they correspond to mean values of the microscopic parameters.

In addition to these structural irregularities, observation of a time-dependent shift in transient absorption spectra (Visser et al., 1995) has indicated that, even at room temperature, spectral differences between individual pigments (inhomogeneous broadening) may play a role. Earlier, these effects were only observed at cryogenic temperatures (Timpmann et al., 1991). In this paper we assume that the effects of spectral heterogeneity on the overall exciton lifetime can be ignored at room temperature. If necessary, they can be described by perturbation approaches that were pre-

viously applied for intermediate temperatures (Somsen et al., 1994; Valkunas et al., 1994).

Although the paragraphs above indicate that a regular lattice model may reproduce the exciton decay kinetics, a rather large number of microscopic parameters is required even to describe the exciton kinetics in the relatively simple photosynthetic system of *Rs. rubrum*. It is important to determine how these parameters affect the overall kinetics, and for this purpose some kind of analytical approximation of the exciton kinetics is necessary. Previously, the RC was modelled as a local perturbation of a homogeneous lattice by two groups who investigated the integrated exciton population (Hemenger et al., 1972; Pearlstein, 1982) and the longest time kinetics (Valkunas et al., 1986; Kudzmauskas et al., 1983). We demonstrate in Theory, that these approaches are similar and exploit this to obtain additional information about the exciton decay process. However, both approaches fail when energy migration within the LHA is fast in comparison to its delivery to the RC, especially when the LHA is small. We develop an alternative model by regarding this finite migration as a perturbation instead. These approaches are compared to numerically simulated kinetics of small systems ($\leq$ 64 sites), and in Analysis they are applied to investigate room temperature kinetics in *Rs. rubrum* and to obtain information about the structural organization of LH1 core antenna in this bacterium. Preliminary conclusions can be drawn on the amount of clustering of the pigments and on the pigment orientations.

THEORY

At sufficiently low excitation light intensities, the excited state kinetics of an LHA complex of N pigments can be expressed in the time dependent populations x_n of site $n = 0, \cdots, N-1$, which satisfy:

$$\frac{dx_n}{dt} = \sum_{m=0}^{N-1} W_{nm}x_m \quad \text{or} \quad \frac{dx}{dt} = Wx \tag{1}$$

where W_{nm} is the rate of transfer from pigment m to n, W_n the decay rate from pigment n, and $W_{nn} = -W_n - \sum_{m\neq n} W_{mn}$ represents the total transfer rate away from site n. The $N \times N$ rate matrix W has N negative eigenvalues λ_n that correspond to the decay rates. However, experimental kinetics typically show only the slowest decay (λ_0) from a semi-equilibrium state. The other eigenvalues represent rapid equilibrations that are not only much faster, but also have a small amplitude, e.g., $\approx(\lambda_0/\lambda_n)^2$ in homogeneous lattices.

Local trap models

Hemenger et al. (1972) proposed to study exciton quenching on a lattice with traps by means of the zeroth moment of the total population, which is an estimate of the decay time in the case of approximately monoexponential decay (Pearlstein, 1982; Knox, 1968):

$$M_0 = \int_0^\infty \left(\sum_{n=0}^{N-1} x_n(t)\right) dt \approx \int_0^\infty e^{-t/\tau}\, dt = \tau \tag{2}$$

On a regular lattice where the trap is modeled by a decay rate γ on pigment $n = 0$ and transfer rates W_T and W_D to and from this site respectively, M_0 was expressed analytically. The most elegant form (Pearlstein (1982), Eq. 15) is obtained with restriction to nearest neighbor transfer and homogeneous excitation of the LHA ($x_n(t) = \delta_{n0}\rho_{RC} + (1 - \delta_{n0})\rho_{RC}$):

$$\begin{aligned} M_0(\rho_{RC}) &= \tau_Q + (1 - \rho_{RC})(\tau_T + \tau_{mig}) \\ &\equiv \tau_Q + (1 - \rho_{RC})\tau_{FP} \end{aligned} \tag{3}$$

where τ_{mig} and τ_T can be regarded as the times needed for migration through the LHA and to the RC, and τ_Q as the average time needed to quench the exciton after that:

$$\begin{aligned} \tau_Q &= \frac{W_T + W_D(N-1)}{W_T}\frac{1}{\gamma} \\ \tau_T &= \frac{N-1}{z}(W_T^{-1} - W_h^{-1}) \qquad \tau_{mig} = \frac{N^2}{N-1}h_d(N)W_h^{-1} \end{aligned} \tag{4}$$

Besides the coordination number z (i.e., the number of neighbors to each pigment) and the dimension d, the only dependence on the LHA lattice is included through the structure function $h_d(N)$ in the migration time τ_{mig} (see Eq. A7). Its value is shown in Fig. 1 for a variety of LHA structures and varies only mildly over a range of lattice sizes, except for linear arrays. The expression for M_0 can be used directly to analyze fluorescence experiments. If the radiative lifetime of all sites is equal to τ_F, the quantum yield (QY) is $QY = M_0/\tau_P$. This result may be applied to obtain the "escape" ratio (α) of fluorescence quantum yield after selective excitation of the RC and the LHA respectively, as described in the introduction:

$$\alpha = \frac{QY_{RC}}{QY_{LHA}} = \frac{M_0(1)}{M_0(0)} = \frac{\tau_Q}{\tau_Q + \tau_{FP}} \tag{5}$$

On the other hand, M_0 cannot always be used to estimate the exciton lifetime (τ). Especially in small systems if τ_{FP} is larger than τ_Q, M_0 shows considerable ρ_{RC} dependence; whereas the exciton lifetime depends only on the rate matrix, and not on initial conditions.

An explicit description of the exciton decay times was developed by Valkunas, Kudzmauskas, and Liuolia (Kudzmauskas et al., 1983; Valkunas et al., 1986). By means of the Green's function formalism for the same LHA lattices as discussed above, an equation for the N decay times corresponding to the eigenvalues of the rate matrix was obtained (see Appendix A, Eq. A4 or Valkunas et al. (1986), Eq. 25), which allows a graphical analysis. Although the equation cannot be solved analytically, the au-

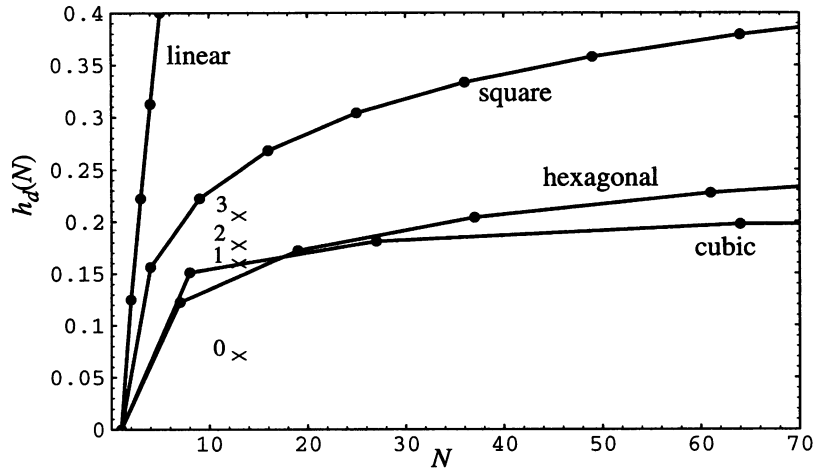

FIGURE 1 The structure function $h_d(N)$ plotted against the LHA size (N). The drawn curves represent one- (linear), two- (square, hexagonal), and three-dimensional (cubic) LHA lattices (with periodic boundary conditions). The crosses mark an LHA structure of 12 sites on a ring around the RC. In the bottom case, transfer between the RC and all sites is included. In the other cases, six sites are connected to the RC. The connected sites clustered in groups of one, two, or three sites.

thors obtained an approximation for large LHAs by ignoring all terms of order τ^2 and 1/N. In smaller systems this is not correct, but an alternative approximation can be obtained by expressing τ as a power series in γ (see Eq. A11):

$$\tau = M_0\left(\frac{W_T}{W_T + W_D(N-1)}\right) + O(\gamma) \equiv M_0(\rho_{EQ}) + O(\gamma) \tag{6}$$

Remarkably, this approximation of the longest lifetime can be expressed in terms of M_0 by setting $\rho_{RC} = \rho_{EQ}$ equal to the hypothetical thermal population of the RC. The fact that both the average and the longest lifetime are given by one expression makes the estimates more reliable. Although the exciton kinetics is neither purely "sequential" nor purely "parallel," the exciton lifetime is approximately as a sum of three time constants. In Eq. 6, the migration and trapping times are scaled by W_T and W_D. This effect disappears for large systems, in which case an even simpler expression is obtained (Valkunas et al., 1986; Somsen et al., 1994). The analogy between the average and longest lifetime can be taken even further to demonstrate that $\tau > M_0(\rho_{EQ})$ is in fact a lower limit. In most practical circumstances $M_0(0)$ is an upper limit.

Perturbed two-level model

The local trap approaches are correct if the RC has only a localized effect on the exciton kinetics of the LHA. In small ($N \lesssim 10$) systems such as LH1, this may not be the case. However, in such cases the equilibration within the antenna is typically fast and may give rise to an alternative approach. In the limit if infinitely fast migration ($W_h^{-1} = 0$), the LHA behaves as if it were a single supermolecule, because the

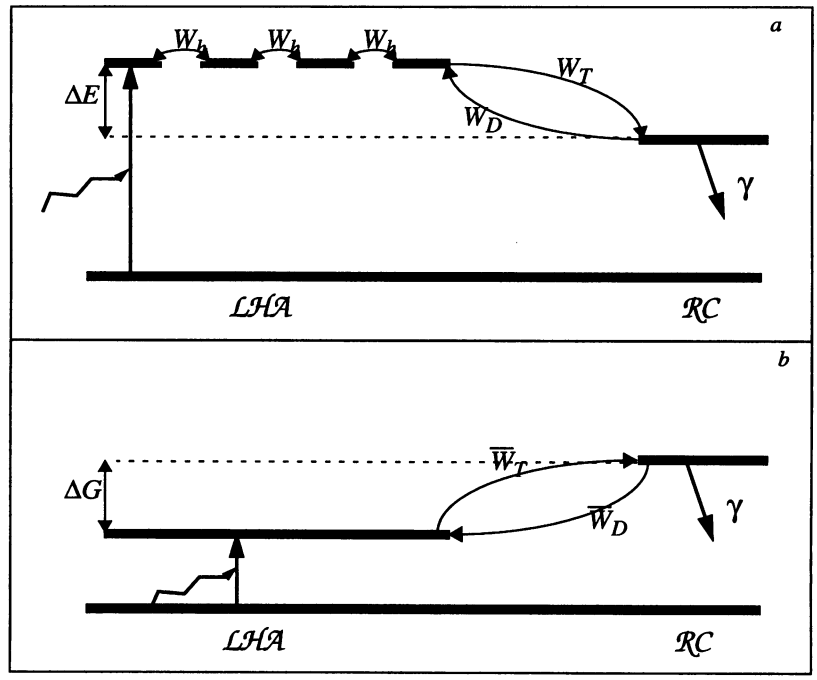

FIGURE 2 Schematic representation of the LHA-RC complex (*a*) and its two-level approximation (*b*) where the antenna is represented by a single level. The transfer rate (W_h) between neighboring sites in (*a*) is no longer regarded in (*b*). The transfer (W_T and W_D) between the RC and its neighboring sites on the LHA, is replaced by overall transfer ($\bar{W}_T$ and W_D) between the levels. The free energy difference (ΔG) is less than the energy difference (ΔE) because the larger number of sites shifts the equilibrium toward the LHA.

population of all sites remains equal. As illustrated in Fig. 2, the exciton kinetics are then reproduced by a model with two levels: one for the LHA and one for the RC. In this model, the finite migration can be included as a perturbation.

Let us first consider the simple two-level model. The exciton kinetics are expressed in terms of the effective transfer rates between the two levels:

$$\bar{W}_T = \frac{1}{N-1}\sum_{n=1}^{N-1} W_{0n} = \frac{zW_T}{N-1}$$
$$\bar{W}_D = \frac{1}{1}\sum_{n=1}^{N-1} W_{n0} = zW_D \tag{7}$$

The second equalities are correct in the case of nearest neighbor transfer, as long as pigment orientations are ignored. The two time constants of this system, corresponding to equilibration ($\tau_+ = -1/\lambda_+$) and exciton decay ($\tau_- = -1/\lambda_-$), are obtained with a single expression:

$$\lambda_\pm = -\frac{\gamma + \bar{W}_T + \bar{W}_D \pm \sqrt{(\gamma + \bar{W}_T + \bar{W}_D)^2 - 4\gamma\bar{W}_T}}{2} \tag{8}$$

In addition, the escape ratio of the fluorescence quantum yield after homogeneous excitation of the RC and the LHA, respectively, is equal to:

$$\alpha = \frac{QY_{RC}}{QY_{LHA}} = \frac{\bar{W}_T + \bar{W}_D}{\gamma + \bar{W}_T + \bar{W}_D} \tag{9}$$

Based on these results we can now consider the case of finite migration by expressing the exciton lifetime as a power series in W_h^{-1}. This procedure is discussed in Appendix B. It requires careful consideration, because the rate matrix W is singular at $W_h^{-1} = 0$. The two time constants are then expressed as (see Eq. B13):

$$\tau_\pm(W_h^{-1}) = -\frac{1}{\lambda_\pm} + (N-1)\frac{\bar{W}_T\bar{W}_D}{(\bar{W}_T + \lambda_\pm)^2 + \bar{W}_T\bar{W}_D} \times g_d(N)W_h^{-1} + O(W_h^{-2}) \tag{10}$$

A similar refinement may be obtained for the escape ratio. The function $g_d(N)$ is defined in Eq. B12 and relates only to the structure of the LHA. It is equivalent to the structure function $h_d(N)$ of the local trap model. The two-level structure function is plotted in Fig. 3 for various lattice organizations.

Although they are different in nature, qualitative comparisons can be made between the perturbed two-level approximation and the two local trap approximations discussed above. In both cases, a migration time proportional to W_h^{-1} can be separated out. This migration time is not completely independent of the RC, but the correction appears as a scaling factor, which is in all cases smaller than but near to unity. The trapping time, obtained as τ_- in the two-level model, cannot in general be expressed as the sum of the times needed for delivery to and quenching by the RC. However, this property changes for large N. In that case $\bar{W}_T$ becomes arbitrarily small, and Eq. 10 reduces to:

$$\tau_\pm \approx \frac{\bar{W}_D}{\bar{W}_T}\frac{1}{\gamma} + \frac{1}{\bar{W}_T} + Ng_d(N)W_h^{-1} \tag{11}$$

This compares very well with the result in Eq. 4 and explains some of the differences between the two structure functions. In Eq. 4, τ_T is expressed as the perturbation of the delivery time and includes a contribution proportional to W_h^{-1}. Alternatively, this contribution can be included in the migration time, as is effectively done in the perturbed two-level approximation. In that case an offset is subtracted from the structure function $h_d(N)$, which makes it more comparable to $g_d(N)$.

In Fig. 4, the exciton lifetimes predicted by the local trap (Eq. 6) and perturbed two-level approximations (Eq. 10) are compared with numerical results for square LHA lattices. A simplified local trap approximation (Valkunas et al., 1986; Somsen et al., 1994) is added for illustration. The local trap approximation becomes accurate for LHAs with more than 30 or so pigments. They are less accurate if trapping or detrapping is slower than hopping within the LHA. The perturbed two-level approximation is cor-

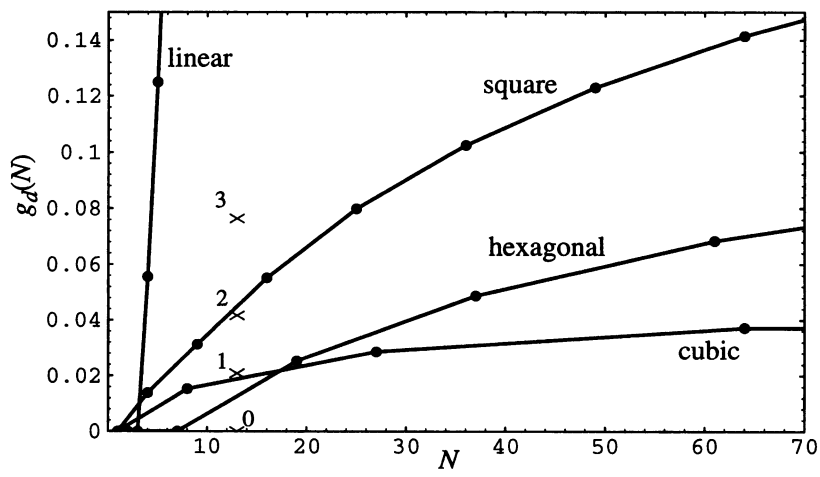

FIGURE 3 The two-level structure function $g_d(N)$ plotted against the LHA size (N). The drawn curves represent one- (linear), two- (square, hexagonal), and three-dimensional (cubic) LHA lattices (with periodic boundary conditions). The crosses mark a LHA structure of 12 sites on a ring around the RC. In the bottom case transfer between the RC and all sites is included. In the other cases, six sites are connected to the RC. The connected sites clustered in groups of one, two, or three sites.

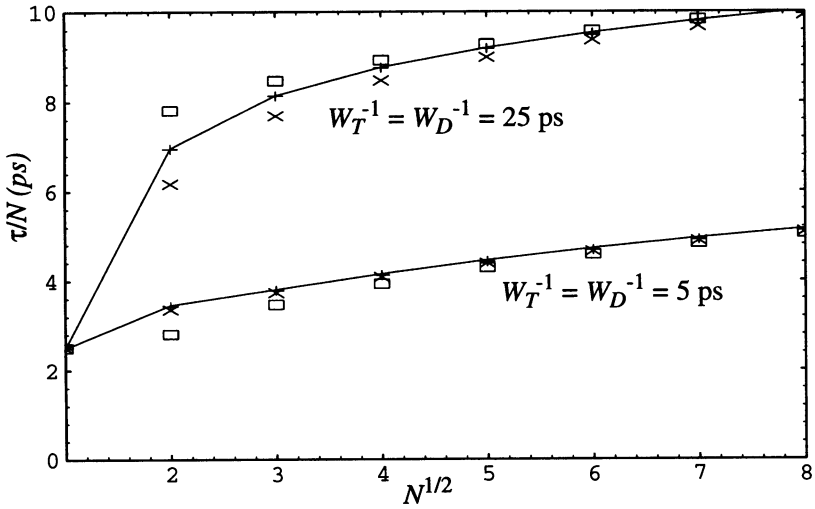

FIGURE 4 The effect LHA-size and magnitude of the perturbation W_T,W_D on the approximations for the exciton lifetime. Shown is the exciton lifetime, divided by the LHA-size (N) as a function the length ($N^{1/2}$) of its sides. As described in the text, numerical results (*connected points*) are compared to those of the normal (×) and simplified (□) local trap model and the two-level model (+). In each calculation γ^{-1} = 2.5 ps, whereas two different values are used for $W_T^{-1} = W_D^{-1}$ as indicated in the plot. An unusually slow value for the hopping rate (W_h^{-1} = 10 ps) was used for illustration purposes.

rect in small as well as large LHAs, and a large overlap exists where both approximations can be used successfully. To further test the approximations, simulations were carried out on a 4 × 4 LHA lattice with a range of values for W_T, W_D, and W_h (data not shown). At the expense of a more complicated expression, the perturbed two-level approximation is in all cases superior to the local trap approximation. In some cases, Eq. 10 breaks down for $W_D < W_T$ and can be improved by using $M_0(1/N)$ instead.

Finally, simulations were carried out for ring-shaped models (data not shown). The accuracy of the approximations was similar to those in the square lattice, even though the theoretical description of the local trap is not valid for such models.

ANALYSIS

With the tools developed above, we now investigate the relation between kinetics and structure of the LH1 core antenna of *Rs. rubrum*. This is done with the experimental data that were discussed in the Introduction. The exciton lifetime increases from γ^{-1} = 4.5 ps in membrane bound RCs to τ = 60 ps in the presence of the LH1 antenna protein. The escape ratio α (of fluorescence QYs upon selective excitation of the RC and the LHA, respectively) is not unambiguously determined. We adopt the range α = 0.2–0.3 and perform the calculations below for both values.

In this analysis, we assume that the $N - 1 = 12$ pigment dimers in the antenna behave like single sites. Considering the size of the RC and the sixfold symmetry observed in isolated LH1 by electron microscopy (Stark et al., 1983), these must be arranged around the RC either as six groups of two dimers or as twelve separate dimers.

For the rate of hopping between neighboring sites, we adopt the value W_h^{-1} = 0.65 ps, obtained by analysis of singlet-singlet annihilation with a two-dimensional model (Valkunas, 1989; Trinkunas and Valkunas, 1989; Valkunas et al., 1995). This may not be correct if the organization is a one-dimensional ring, as in the single PSU; but it is a reasonable estimate if we assume that fast transfer takes place between neighboring PSUs, because this partially restores the two dimensional nature of the lattice.

In the following, the structure-kinetics relation is analyzed with the local trap and the perturbed two-level approximation. This analysis is done in two steps. First, the average rate of transfer between the LHA and the RC is estimated. This can be done with few assumptions about the structure. Second, this average rate is interpreted in terms of more detailed structural models.

Local trap approximation

The data above may be analyzed with the combined results of the averaged and the longest lifetime approach. First we consider from Eq. 5 that:

$$\alpha = \frac{\tau_Q}{\tau_Q + \tau_{FP}} \Leftrightarrow \frac{\tau_{FP}}{\tau_Q} = \frac{1-\alpha}{\alpha} = 4 - 2.3 \qquad (12)$$

Apparently, the low escape ratio implies that the excited state decay in the PSU is limited by the first passage time. This can be further evaluated by rewriting Eq. 6:

$$\tau \approx M_0(\rho_{eq}) = \tau_Q + \left(1 - \frac{\gamma^{-1}}{\tau_Q}\right)\tau_{FP} \Leftrightarrow \tau_Q = \alpha\tau + (1-\alpha)\gamma^{-1} \qquad (13)$$

Again, the value of α determines whether the kinetics is limited by τ_{FP} or by τ_Q. From Eqs. 12 and 13, we estimate τ_Q = 16–21 ps and τ_{FP} = 62–49 ps. From, the quenching time (τ_Q), the thermal equilibrium population of the RC can directly be obtained (see Eq. 4). The estimate ρ_{EQ} = 0.29–0.21 is somewhat larger than $1/N$, which indicates that the RC may be red shifted by 26–20 nm with respect to the main band of the LHA. Note that this refers to the positions

of the zero phonon lines, and not necessarily to the maxima of the absorption bands.

The first passage time is the sum of the time needed for migration in the LHA and transfer to the RC ($\tau_{FP} = \tau_{mig} + \tau_T$, see Eq. 4). To estimate the former, we consider a hexagonal lattice with the values $N - 1 = 12$ and $W_h = 0.65$ ps, so that $h_a(N) = 0.12$ (see Fig. 1) finally yields $\tau_{mig} = 1.1$ ps. Other lattices lead to similar values. This indicates that the first passage time is largely determined by τ_T, and the effective trapping rate (defined in Eq. 7) can be estimated $\bar{W}_T^{-1} = (zW_T/(N-1))^{-1} = 63$–$50$ ps. Surprisingly, the first value is slightly larger than τ itself. This may be related to the deterioration of the approximation in slow detrapping cases, as was discussed in the simulations. This can be avoided by using $M_0(1/N)$ as an approximation for τ, which indeed leads to slightly smaller estimates for $\bar{W}_T^{-1}$ (not shown). Individual trapping rates W_T can only be obtained if the coordination number (z) is known. For a 12-fold symmetric PSU, $z = 12$, but its number varies considerably for any other arrangement of the LHA sites. This will be discussed below.

Finally, let us consider how the estimates of $\bar{W}_T$ and ρ_{EQ} depend on the experimental parameters. Because of the fast hopping, $\bar{W}_T$ is virtually independent of W_h as well as N. The estimate of ρ_{EQ} is also independent of these parameters. The sensitivity of $\bar{W}_T$ to γ is limited to the small effect in Eq. 13. The effect on ρ_{EQ} and consequently the red shift of the RC is somewhat larger. The relation of exciton lifetime and escape ratio to the effective rates of trapping and detrapping is illustrated in Fig. 5. The detrapping rate $\bar{W}_D = zW_D$ depends strongly on α, but is almost independent of the actual value of τ. In contrast, $\bar{W}_T^{-1}$ scales approximately proportional to τ and depends only mildly on α.

Perturbed two-level approximation

A similar analysis is possible with the two-level model. This model is implicitly expressed in terms of the effective rather than individual transfer rates, and requires no additional assumptions to estimate these parameters.

First, we consider the migration component to the exciton lifetime (see Eq. 10). It vanishes if trapping to the RC occurs equally fast from all LHA sites; but in practice, some amount of migration is present, because asymmetry of the RC favors transfer to and from a subset of the LHA sites. We include this by assuming that only two groups of three sites on either side of the ring of LHA sites are connected to the RC (case 3 in Fig. 3). Although Eq. 10 depends on several, as yet unknown, parameters, an upper limit of the migration component is simple to obtain. The two-level structure function is $g_d(N) = 0.08$; and with $N - 1 = 12$ and $W_h^{-1} = 0.65$ ps, the migration component is faster than 0.6 ps. Because other structural models lead to even smaller values, we ignore the migration component in the calculations below.

The kinetics of the two-level models are expressed in Eq. 8 where the exciton lifetime $\tau = -\lambda_-^{-1} = 60$ ps. To get a better impression of the relation between the rate parameters, the equation may be rewritten as:

$$\bar{W}_T = -\lambda_- \left(\frac{\gamma + \bar{W}_T + \bar{W}_D + \lambda_-}{\gamma} \right) \qquad (14)$$

With sufficiently slow trapping and detrapping ($\bar{W}_T + \bar{W}_D \ll \gamma$) the exciton lifetime is limited by trapping, i.e., $\bar{W}_T \approx -\lambda_-$. Whether or not this is the case is determined by the escape ratio. This may be seen by rewriting Eq. 9:

$$\frac{\bar{W}_T + \bar{W}_D}{\gamma} = \frac{\alpha}{1 - \alpha} \qquad (15)$$

from which we obtain directly $(\bar{W}_T + \bar{W}_D)^{-1} = 4$–$2.3\gamma^{-1} = 18$–$10$ ps. A combination of the two equations leads to $\bar{W}_T^{-1} = 51$–44 ps, which is 10–20% faster than the estimates obtained with the local trap approximation above.

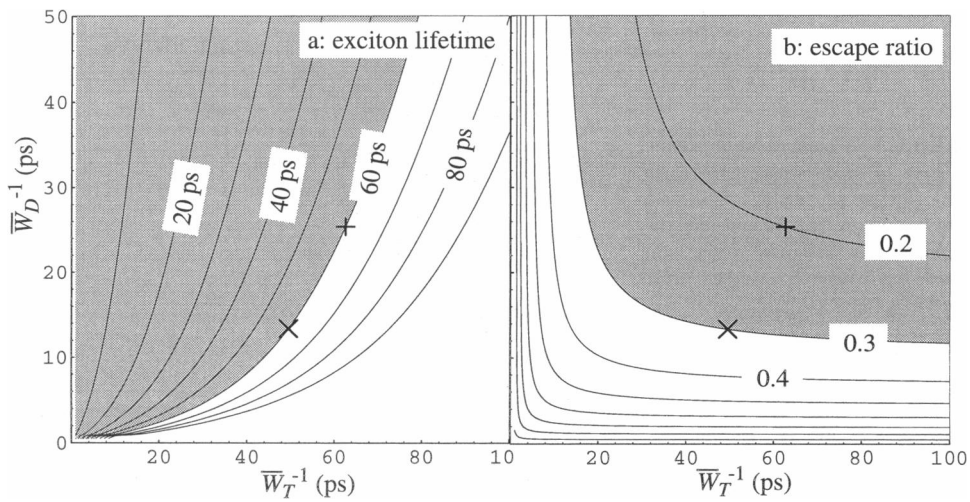

FIGURE 5 Contour plot of exciton lifetime (a) and escape ratio (b) in LH1 ($N = 13$, $z = 6$, $h_d(N) = 0.12$, $\gamma^{-1} = 4.5$ ps, $W_h^{-1} = 0.65$ ps) as a function of trapping and detrapping time, according to the local trap approximation. Marked areas are $M_0(\rho_{EQ}) < 60$ ps and $\alpha < 0.3$. The outcome of our estimate (see text) is marked by "×" ($\alpha = 0.3$) and "+" ($\alpha = 0.2$).

Finally, we consider again how these estimates are affected by the experimental parameters. Because we have ignored the contribution of migration, $\bar{W}_T$ and $\bar{W}_D$ are independent of the value of W_h and also of the value of N. In addition, the estimate of $\bar{W}_T$ is nearly independent of γ, but $\bar{W}_D$ may be strongly affected. The sensitivity of the estimates to τ and α, is investigated in Fig. 6, by displaying them as a function of $\bar{W}_T$ and $\bar{W}_D$ in a contour plot. The plots are similar to those of the local trap model, but show more clearly that the estimate of $\bar{W}_T$ depends only mildly on α. Moreover, $\bar{W}_T^{-1} \leq \tau = 60$ ps poses an upper limit to the effective trapping time, independent of α. $\bar{W}_D$ is determined by α, and especially its lower limit is uncertain if escape ratios smaller than 0.2 are possible.

Interpretation of the effective trapping rate

The results in the previous pages may be summarized by concluding that the effective trapping rate (see Eq. 7) is almost certainly within the range $\bar{W}_T^{-1} = 63$–44 ps. The estimate of the effective detrapping rate ($\bar{W}_D$) is less clear due to the uncertainty of the escape ratio (α). Within reasonable limits, any model that satisfies this condition reproduces the experimentally observed exciton trapping kinetics. This can however be achieved in different ways, and parameters can be varied to comply with other kinetic data. For example, the condition is satisfied if all LHA sites are connected to the RC and deliver excitons at a rate between 63 and 44 ps, but also if only half the sites are connected to the RC at a rate between 32 and 22 ps. In the extreme case that only one site delivers excitons to the RC, a transfer rate of 5–4 ps is required.

In all cases the delivery rates are considerably slower than the transfer between neighboring pigments in the antenna ($\bar{W}_h^{-1} = 0.65$ ps), indicating that the distance (r) from the antenna sites to the (special pair of the) RC is larger than the distance (a) between neighboring sites in the antenna, because of the larger size of the RC protein. Assuming Förster transfer, the first case requires a distance ratio $r/a = (63\text{–}44/0.65)^{1/6} = 2.1\text{–}2.0$, which agrees reasonably well with the organization of 12 sites on a ring around the RC. Nevertheless, various other models deserve a more detailed consideration. For this purpose, a number of factors have to be considered before we can discuss various standardized models.

In Förster's theory (Förster, 1965) the exciton transfer between weakly coupled pigments depends on their positions, orientations and spectral properties. The transfer rate W between two sites at distance r can be expressed as:

$$W = W_0 \frac{\kappa^2}{r^6} f(\Delta) \tag{16}$$

Here, $f(\Delta)$ is the relative ($f(0) = 1$) spectral overlap between the fluorescence spectrum of the donor and absorption of the acceptor as a function of the energetic separation Δ between them. The orientation factor κ^2 is derived from the orientation factor κ for dipole-dipole interaction (see Eq. C1) and varies between 0 and 4. Finally, W_0 is the transfer rate that would have been obtained at unit distance, with $\Delta = 0$ and $\kappa = 1$ (e.g., a sandwich dimer).

Equation 16 can be used to estimate distance ratios provided that transfer rates between individual sites are known. In the simplest case that transfer to the RC occurs from a number of neighboring sites at one fixed rate (W_T), the coordination number (z) of the RC is needed. In the 12-fold symmetric PSU, $z = 12$, if the 12 LHA dimers are grouped in 6 dimer pairs, z can be either 6 or 12 depending on the arrangement; and if asymmetry of the RC limits trapping to only one or a few sites, the coordination number may even decrease down to $z = 1$. In each case W_T can be calculated with Eq. 7.

A more refined estimate is obtained by considering that, notwithstanding the strong distance dependence, a relevant amount of trapping may still occur from sites farther away from the RC. This can be corrected for by using an effective coordination number that includes these sites, scaled by the sixth power of their relative distance to the RC.

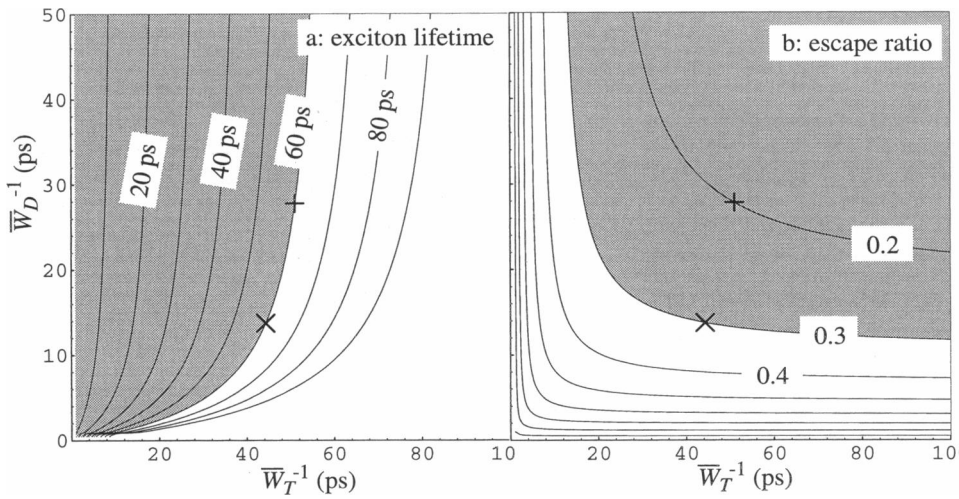

FIGURE 6 Contour plot of exciton lifetime (a) and escape ratio (b) in LH1 ($\gamma^{-1} = 4.5$ ps, $W_h^{-1} = 0$) as a function of effective trapping and detrapping time, according to the two-level approximation. Marked areas are $M_0(\rho_{EQ}) < 60$ ps and $\alpha < 0.3$. The outcome of our estimate (see text) is marked by "×" ($\alpha = 0.3$) and "+" ($\alpha = 0.2$).

Secondly, the orientation factors κ^2 may be taken into account, because these cause considerable variation of the transfer rates from individual LHA sites to the RC. The approaches above yield the average transfer rate over all z neighboring sites to the RC and must be analyzed with the average orientation factor $\langle\kappa^2\rangle$. Its value is calculated in Appendix C for a ring of LHA sites with the RC in the origin. If all transition dipole moments are parallel to the plane of the ring, and the transition dipole moment of each LHA site is at a fixed angle (ϕ) with its position vector, the average orientation factor in such models is (see Eq. C4):

$$\langle\kappa^2\rangle = \frac{1 + 3\cos\phi^2}{2} \tag{17}$$

Its value is independent of the number of LHA sites and the orientation of the RC, but increases by a factor of 4 when the pigment orientation changes from tangential ($\phi = \pi/2$) to radial ($\phi = 0$). As discussed in Appendix C, the variation with ϕ is reduced if there is a vertical separation between RC and the LHA sites. For transfer within the LHA we assume the value $\langle\kappa_h^2\rangle = 5/4$, obtained by averaging over all configurations in a plane.

As a further refinement, $f(\Delta)$ may be somewhat larger than unity because the negative energetic separation that we obtained earlier in this section is favorable for the spectral overlap. This is not included in the calculations below, which leads to a slight underestimation of the distance ratio r/a. Other factors such as dielectric constants and homogeneous bandwidths are included in W_0 in Eq. 16. Because the LHA sites as well as the (special pair of the) RC are composed of a Bchl a dimer, W_0 is assumed equal for all interactions.

Comparison to standardized models

With the considerations above, Eq. 16 can be applied to estimate the distance ratio:

$$\frac{r}{a} = \sqrt[6]{\frac{\langle W_T\rangle^{-1} W_0 \langle\kappa^2\rangle f(\Delta)}{\langle W_h\rangle^{-1} W_{0h}\langle\kappa_h^2\rangle f_h(0)}} \approx \sqrt[6]{\left(\frac{\langle W_T\rangle^{-1}}{\langle W_h\rangle^{-1}}\right)\left(\frac{\langle\kappa^2\rangle}{\langle\kappa_h^2\rangle}\right)} \tag{18}$$

from the kinetic parameters. The index "h" in the denominator denotes the parameters for hopping within the LHA. The averages in the numerator are taken over the neighboring sites of the RC. The average trapping rate $\langle W_T\rangle$ is obtained from $\bar{W}_T$ and the coordination number. This analysis can be carried out for various models, and then compared with the actual distance ratio within such a model. Four standardized models are illustrated in Fig. 7. In (*a*) the 12 pigment dimers are symmetrically distributed on a ring around the RC. In (*b*) and (*c*) the dimers are grouped in six pairs. Two extreme cases are shown where the dimer pairs are organized either tangentially (*b*) to the ring around the RC or radially (*c*). To characterize the paired nature, the ratio of the intra- and interpair distance is varied between 0.3 and 0.6. The monocoordinate model is illustrated in (*d*).

The analysis of the exciton lifetime is carried out in Table 1. For each model, the effective coordination number is evaluated, which leads to the individual trapping rates, averaged over the nearest neighbors around the RC. The

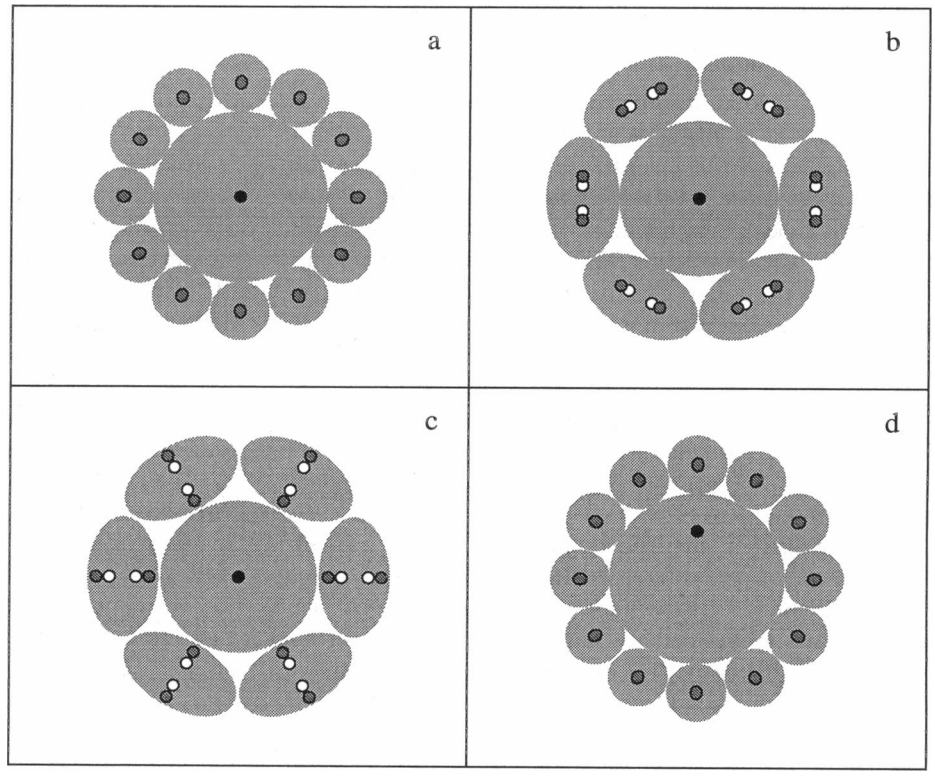

FIGURE 7 Four schematic models for the LH1 core antenna of *Rs. rubrum*. See Table 1 and accompanying text. Central circle in each case is the RC protein with the special pair (the site that actually accepts the exciton) represented by a black disk. Grouped around it are the LHA proteins. In models (*a*) and (*d*) the LHA sites are represented by a gray dot. In models (*b*) and (*c*) the LHA sites are grouped in pairs. The two extreme cases of the distances between sites within a pair are represented by two gray and white disks respectively. The gray ellipses in (*b*) and (*c*) mark the relative area of the RC- and LHA-polypeptide, estimated from the number of transmembrane helices (4 in each pair of LHA units and 11 in the RC).

TABLE 1 Estimated distortion of antenna by RC

Model	z	$\langle W_T \rangle^{-1}$ (ps)	Estimated r/a		Model r/a
			$\phi = 0$	$\phi = \pi/2$	
12-Fold symmetry	12	63–44	2.3–2.2	1.8–1.7	1.9
Six-pair, tangential (0.3–0.6)	12	63–44	2.1–1.9	1.6–1.5	1.2–1.4
Six-pair, radial (0.3–0.6)	6.4–7.2	38–23	1.9–1.8	1.5–1.4	1.0–0.9
Mono-coordinate RC	1	5–4	1.3–1.2		<1.9

distance ratio r/a is then estimated with Eq. 18 for two orientations of the transition dipole moments either parallel ($\phi = 0$) or perpendicular ($\phi = \pi/2$) to the radius of the ring. In model (*d*) the orientation factor is assumed equal to that for hopping. In models (*b*) and (*c*) a hopping rate twice as slow ($W_h^{-1} = 1.3$ ps) is assumed, as a rough compensation for the faster singlet-singlet annihilation in such paired structures. In the last column of Table 1, the distance ratio is calculated for each model in Fig. 7. In models (*b*) and (*c*) the lattice spacing a is replaced by an effective pair-pair distance, which reproduces the average transfer between the pairs.

As illustrated in the first row of the table, the distance ratio in the 12-fold symmetric model falls within the limits estimated from the data. It indicates that all transition dipole moments are tangential along the ring around the RC or at a small angle with it.

The dimer pair models are investigated in the second and third rows. The estimated distance ratios are somewhat smaller than for the 12-fold symmetric model because of the smaller coordination number (third row) and the corrected value used for the hopping rate (second and third rows). However, the models in Fig. 7, *b* and *c* lead to considerably smaller distance ratios. In the presented form, these models do not agree with the kinetic data. In the tangentially organized model (*b*), the difference between the estimated and model values is not too large and may be repaired by further increasing the ratio of the intra- and interpair distances. In that case, the model becomes more similar to the 12-fold symmetric model, but may differ from it because the orientation of the two dimers in a pair is not necessarily the same. However, both dimers must be oriented more or less tangentially with respect to the ring around the RC. A purely radially organized model (*c*) cannot be reconciled with the kinetic data. This conclusion is confirmed by the estimated size of the LHA polypeptide, relative to that of the RC. As illustrated in Fig. 7 *c*, the radially organized model requires the pigments to be positioned too near to the outer edge of the polypeptide.

For comparison, the monocoordinate RC model is investigated in the fourth row of Table 1. In the most extreme case, relatively fast trapping occurs from one LHA site, which allows a considerably smaller distance between the RC and its neighboring LHA site. Only an upper limit of the distance ratio r/a is obtained from the model in Fig. 7 *d*. If the monocoordinate behavior is caused by positioning of the RC site, it must be placed approximately halfway between the LHA pigments and the center of the ring. However, in such a case additional trapping will occur from other LHA sites, which complicates the calculation. A monocoordinate model can also be realized by polarizability changes in the medium between the RC and a selected LHA site. This model was more extensively discussed by Pearlstein et al. (1992).

SUMMARY AND DISCUSSION

In this paper, we have discussed models for exciton trapping in structurally heterogeneous photosynthetic systems and applied these to the LH1 core antenna of photosynthetic purple bacteria. We focused on the distortion of the antenna (LHA) lattice by the presence of a large RC, and included cases of small ($N \lesssim 10$ sites) PSUs. The investigation is mainly based on: 1) comparison of the overall exciton lifetime to kinetic time constants observed within the LHA and the RC, and 2) the observed escape ratio of fluorescence quantum yields upon selective excitation of the RC and the LHA respectively.

Two theories that model the trap as a local perturbation of a homogeneous lattice (Hemenger et al., 1972; Valkunas et al., 1986) were compared and adapted to small PSUs. The exciton lifetime is a sum of three contributions related to migration in the LHA, trapping to the RC, and charge separation in the RC. The first two contributions are scaled by $(1 - \rho_{RC})$, where ρ_{RC} is either the initial population of the RC or its thermal population (ρ_{EQ}), depending on whether the average lifetime or an approximation of the slowest decay component is calculated. The scaling can be appreciable in small PSUs, which indicates that the perturbation by the RC is no longer local in such systems, but affects the entire PSU. Numerical simulations indicate that the approximation is accurate when $\rho_{EQ} < 1/N$. If it is larger, a better approximation is obtained by setting $\rho_{RC} = 1/N$.

An alternative model was explicitly developed for small PSUs where migration is fast, and thus the exciton population of all LHA sites is approximately equal. In first approximation, the PSU is modeled by two levels: one for the LHA and one for the RC. This is refined by including the finite migration rate as a perturbation. Again, the exciton lifetime contains a migration component, but the trapping and charge separation can no longer be separated and lead to a single nonlinear expression. Numerical simulations indicated that the exciton decay kinetics in PSUs of intermediate size ($N = 20$–50) are accurately approximated by this perturbed two-level approach as well as by the local trap approach. In combination, they cover the entire range from very small to very large PSUs.

Both approaches were used independently to investigate the exciton decay kinetics of the LH1 core antenna of *Rs. rubrum* at room temperature. With few assumptions about the structure, the effective rates of trapping ($\bar{W}_T$) to and detrapping ($\bar{W}_D$) from the RC were estimated. Because $\bar{W}_T$ and $\bar{W}_D$ are slow with respect to the charge

separation rate, the excitation lifetime (τ = 60 ps) is limited by the trapping process. More detailed calculations yield $\bar{W}_T^{-1}$ = 63–44 ps and a less certain estimate of $\bar{W}_D$. This functions as a constraint for more detailed models that include the number of sites in the PSU, the coordination number of the RC, and orientation and clustering of pigments. In any case, the transfer between the RC and its neighboring sites in the LHA is considerably slower than the transfer between neighboring sites in the LHA (W_h^{-1} = 0.65 ps). This could be explained by an equidistant distribution of the $N - 1 = 12$ pigment dimers of the LHA that are on a single ring around the RC, provided that the transition dipole moments of the LHA pigments are approximately tangential to the ring. This orientation is the same as in the recently observed structure of LH2 of *Rps. acidophila* (McDermott et al., 1995). An alternative model contains a pair of pigment dimers as its basic building block. It requires, however, that all dimers are more or less on a single ring around the RC. Also in this model, the transition dipole moments are necessarily tangential to the pigment ring.

The conclusions above are based on a comparison of transfer between LHA and RC with the hopping time within the LHA; and their strength depends on the accuracy of these parameters. Firstly, the estimate of the effective trapping rate $\bar{W}_T$ is reliable because this parameter limits the exciton lifetime. In all models, the migration time contributes less than 2%; and the limitedness was further demonstrated by the two-level approximation and is in agreement with the observed low value of the escape ratio (α = 0.2–0.3).

The conclusion that the exciton lifetime is limited by the delivery of excitons to the RC was also drawn from time resolved measurements on site-specific RC mutants of *Rb. sphaeroides* (Beekman et al., 1994). The charge separation rate increased from 3.5 ps in wild-type up to 15 ps in the mutants, but the overall exciton lifetime increased by no more than 30% from 46 ps to 60 ps. Let us discuss this data with the perturbed two-level model. For the wild-type, we assume that the escape ratio is similar to that in *Rs. rubrum*, and Eqs. 14 and 15 lead to the estimate $\bar{W}_T^{-1}$ = 39–34 ps and $\bar{W}_D^{-1}$ = 22–11 ps. The latter values are in close agreement with Beekman et al. (1994). If the same parameters are used for the mutant, the estimated exciton lifetime is τ = 73–91 ps, which is considerably longer than the observed lifetime. This discrepancy is related to the presence of a charge recombination rate of 225 ps, which gives rise to a slow phase in the exciton decay in the mutants. With such a model, the exciton decay becomes an equilibration process, and its rate is obtained by summing those of the forward and backward process: τ' = 55–65 ps, which is in better agreement with the experiment. Without this correction, the perturbed two level model can only be used if the charge recombination is slow with respect to the uncorrected τ, i.e., if the slow exciton decay phase is absent.

The second important parameter is the hopping rate, for which we used the estimate that was obtained earlier from the analysis of singlet-singlet annihilation on a regular lattice (Valkunas, 1989; Trinkunas and Valkunas, 1989; Valkunas et al., 1995). This analysis may, however, be affected by structural details in the small LH1 core particle. Although its value was corrected for the presence of dimer pairs, it may be necessary to re-analyze the annihilation experiments with more detailed structural models, especially for isolated core particles that have a one-dimensional organization of their sites.

Finally, the coordination number of the RC and the number of LHA sites are crucial parameters in the analysis of the exciton trapping. In this paper, the LH1 core antenna is modelled by 12 weakly coupled pigment dimers, in accordance with triplet-minus-singlet spectra (van Mourik et al., 1991; Visschers et al., 1991), but delocalization over larger pigment clusters has been proposed (Dracheva et al., 1994). The analysis of kinetic data within such systems requires a more detailed model for transfer between delocalized states; but by tentative analogy to the case of rapidly equilibrating clusters, they most likely require a relatively slow hopping between the pigments at the cluster edge. This is possible if the clusters are physically separated, but for clusters with more than two or at most four pigments, this is difficult to realize within a symmetric model. Whether or not this delocalization occurs depends on the balance between energetic disorder and interaction strengths.

In addition, recent high resolution electron microscopy of reconstituted PSUs (Karrasch et al., 1995) indicates that these PSUs may contain 32 pigments instead of 24. Such a model dictates an even larger ratio of the rates of trapping and hopping than was obtained in the analysis, which is not in line with the present analysis. This difference can be reconciled if transfer within the ring is in some way less favorable than transfer to the RC.

The models developed in this paper can be applied to various photosynthetic light harvesting systems. Their main advantage is that they allow flexibility in the rates of transfer between the RC and its surroundings. The perturbed two-level model does not require a regular LHA lattice and can be applied as long as the PSU is sufficiently small to describe the migration within the antenna as a perturbation. The local trap models are applicable to larger PSUs. In principle they require a regular lattice structure for the LHA, but numerical simulations indicate that accurate approximations of the exciton lifetime can also be obtained in less symmetric lattices. As yet, there is no theoretical basis for this.

APPENDIX A

The trap as a local perturbation of a lattice

In this appendix, we discuss the approximation that Valkunas, Kudzmauskas, and Liuolia (Kudzmauskas et al., 1983; Valkunas et al., 1986) derived for the longest exciton decay time (τ), i.e., the smallest eigenvalue, of a homogeneous lattice that is locally perturbed by a trap. We

adapt this approximation for application to smaller lattices. The nomenclature that is necessary for this approximation implicitly illustrates the relation with the expression that Hemenger et al. (1972) derived for the zeroth moment, or time integral, of the exciton population.

The approach requires rotational as well as translational symmetry of the lattice, so that all neighboring sites of the trap are equivalent. This condition is satisfied by square and hexagonal lattices, but not by rectangular lattices. We consider only nearest neighbor transfer and ignore additional loss channels such as fluorescence. If necessary, these can be added afterwards to the exciton decay rate, at least as long as the loss rate is equal for all lattice sites. The rate matrix (W) of the perturbed lattice may separated in two contributions:

$$W = W^0 + U \tag{A1}$$

The rate matrix H^0 of the unperturbed lattice is symmetric and its eigenvalues λ_n can be determined analytically. The perturbation matrix U contains only a few nonzero entries of the form $W_T - W_h$, $W_D - W_h$, and γ. The kinetics of the perturbed lattice is discussed below in terms of the Green's functions:

$$G^0(s) = (s - W^0)^{-1} \quad \text{and} \quad G(s) = (s - W)^{-1} \tag{A2}$$

which are simply the inverse matrices of $s - W^0$ and $s - W$ respectively, where s stands for "s times the identity matrix." The eigenvalues of a matrix are directly related to the singularities of its Green's function. On the other hand, the Green's function is related to the Laplace transform of the exciton population, which converges to its zeroth moment in the limit $s \to 0$. Typically, G^0 and U are known, and the matrix G must be evaluated. This may be done with Dyson's equation:

$$G = G^0 + G^0UG \tag{A3}$$

which is simple to check by substitution of Eq. A2. The Green's function G occurs on both sides of the expression and cannot immediately be obtained. Let us therefore consider the entries G_{00} and G_{x0}, where x represents the neighboring sites to the trap that is arbitrarily set at site $n = 0$. All G_{x0} are equal because of the rotational symmetry of the lattice, and both are functions of s. Because U has few nonzero entries, the evaluation of G_{00} and G_{x0} with Eq. A3 requires only those same two entries on the right-hand side of the equation. This forms a set of two linear equations with two unknowns.

Hemenger et al. (1972) obtained the entire Green's function matrix by the above-mentioned approach. This leads to a complicated expression for the Laplace transform of the exciton population, which transforms to the zeroth moment by taking the limit $s \to 0$.

In contrast Valkunas, Kudzmauskas, and Liuolia (Kudzmauskas et al., 1983; Valkunas et al., 1986) obtained an equation for the eigenvalues s of the perturbed lattice. This requires that G_{00} is singular, and thus that the determinant of the two equations is zero. This leads to Eq. 25 in Valkunas et al. (1986):

$$\begin{aligned} zW_hW_T(\gamma + s)G^0_{00} - (\gamma + s)(W_T - W_h)(1 - sG^0_{00}) \\ + zW_hW_D(1 - sG^0_{00}) = 0 \end{aligned} \tag{A4}$$

With all kinetic parameters known, this is indeed an equation for s. Note that G^{00}_0 itself is also a function of s and may be expressed as:

$$G^0_{00}(s) = \frac{1}{N}\sum_n \frac{1}{s - \lambda_n} = \frac{1}{Ns} + \frac{1}{N}\sum_{n\neq 0} \frac{1}{s - \lambda_n} \tag{A5}$$

The second equality is obtained from the assumption that γ is the only decay channel so that the unperturbed system has a single equilibrium state with eigenvalue $\lambda_0 = 0$. To solve Eq. A4, the authors ignored all terms of order s^2 and $1/N$, which leads to a linear equation for s.

This approach is not correct for small lattices ($N \lesssim 10$). We propose to adapt it by considering γ as a perturbation. It may be checked that for $\gamma = 0$, Eq. A4 has a solution $s = 0$. If sufficiently smooth, the perturbation $s(\gamma)$ of this solution can be expressed as a power series, i.e., up to second order:

$$s(\gamma) = a\gamma + b\gamma^2 + O(\gamma^3) \tag{A6}$$

of which the coefficients a and b should be determined by substitution in Eq. A4. First we substitute Eq. A6 in the individual terms to obtain these as a function of γ up to first order:

$$\begin{aligned} sG^0_{00}(\gamma) &= \frac{1}{N} - \sum_{n\neq 0}\frac{a\gamma}{N\lambda_n} + O(\gamma^2) \equiv \frac{1}{N} + a\frac{h_d(N)}{W_h}\gamma + O(\gamma^2) \\ \gamma G^0_{00}(\gamma) &= \frac{1}{Na} + \left(-\frac{b}{Na^2} + \frac{h_d(N)}{W_h}\right)\gamma + O(\gamma^2) \end{aligned} \tag{A7}$$

where the structure function $h_d(N)$ depends only on the unperturbed lattice. By substitution in Eq. A4 its zeroth and first order terms in γ are obtained:

$$\begin{aligned} 0 = {} & \frac{zW_h(W_T(a+1) + W_D(N-1)a)}{Na} \\ & + \frac{1}{N}\Big[-zW_hW_T\frac{b}{a^2} + zW_TN(a+1)h_d(N) \\ & - (a+1)(W_T - W_h)(N-1) \\ & - zW_Dah_d(N)N\Big]\gamma + O(\gamma^2) \end{aligned} \tag{A8}$$

This equation can only be satisfied if both terms are zero. The former requires:

$$a = -\frac{W_T}{W_T + W_D(N-1)} \tag{A9}$$

and the latter:

$$\begin{aligned} \frac{b}{a^2} &= -(a+1)\left(\frac{1}{zW_h} - \frac{1}{zW_T}\right)(N-1) \\ &\quad + \left(\frac{W_T(a+1) - W_Da}{W_T}\right)\frac{h_d(N)}{W_h}N \\ &= \frac{W_D(N-1)}{W_T + W_D(N-1)}\left(\frac{1}{zW_T} - \frac{1}{zW_h}\right)(N-1) \\ &\quad + \frac{W_D}{W_T + W_D(N-1)}\frac{h_d(N)}{W_h}N^2 \end{aligned} \tag{A10}$$

This, gives an expression for the slowest decay rate s, or instead the exciton lifetime:

$$\begin{aligned} \tau &= -\frac{1}{s} = -\frac{1}{a\gamma} + \frac{b}{a^2} + O(\gamma) \\ &= \frac{W_T + W_D(N-1)}{W_T}\frac{1}{\gamma} + \frac{W_D(N-1)}{W_T + W_D(N-1)} \\ &\quad \times \left(\frac{N-1}{z}\left(\frac{1}{W_T} - \frac{1}{W_h}\right) + \frac{N^2}{N-1}h_d(N)\frac{1}{W_h}\right) + O(\gamma) \end{aligned} \tag{A11}$$

This expression is identical to $M_0(\rho_{EQ})$, as demonstrated in Eq. 6.

APPENDIX B

The perturbed two-level model

In this appendix, an approximation is developed that describes exciton quenching by a trap in a relatively small lattice ($N \lesssim 10$). In such systems the trap is not a local perturbation, especially if transfer between trap and lattice is slower than within the lattice. On the other hand the fast equilibration within the lattice may be regarded as a perturbation instead.

There are two ways to describe this perturbation. One may start from the case that transfer within the lattice is infinitely fast ($W_h^{-1} = 0$). In that case, the antenna remains at equilibrium and the system is modeled by two levels, one for the trap and one for the lattice. A case of finite equilibration can be described as a "perturbation of the two-level model."

Alternatively, one may start with a lattice with a hole and attach the trap as a perturbation. The two approaches are equivalent, because the rates can be scaled. Below we follow the "attached trap approach," which avoids the singularity of the rate matrix at ($W_h^{-1} = 0$). Nevertheless, the perturbation of the exciton lifetime is linear in the hopping time W_h^{-1}.

First, some aspects of the perturbation approach are considered, because it differs somewhat from the standard approach used in quantum mechanics. Next, the perturbation is evaluated for the LHA model. The first order perturbation leads to the two-level model described in the text, and is obtained without any assumption on the lattice symmetry. The second order perturbation describes the migration within the lattice and requires some symmetry in the connection between the lattice and the trap.

A perturbation approach considers one or more eigenvectors and eigenvalues of a matrix:

$$H = H_0 + \alpha U \tag{B1}$$

The scalar α describes all cases between the unperturbed ($\alpha = 0$) situation and the final perturbation ($\alpha = 1$). The eigenvector and eigenvalue are a function of α, which can be described as a power-series if the functions are sufficiently smooth:

$$Hy = \mu y \quad \text{with} \quad \begin{cases} y = y_0 + y_1\alpha + y_2\alpha^2 + \cdots \\ \mu = \mu_0 + \mu_1\alpha + \mu_2\alpha^2 + \cdots \end{cases} \tag{B2}$$

In the following, we are mainly interested in the eigenvalues, because these correspond to the kinetic rates of the systems. The lowest coefficients of the power-series are obtained by combining Eqs. B1 and B2 into a set of matrix equations:

$$\begin{aligned} H_0y_0 &= \mu_0y_0 \\ H_0y_1 + Uy_0 &= \mu_0y_1 + \mu_1y_0 \\ H_0y_2 + Uy_1 &= \mu_0y_2 + \mu_1y_1 + \mu_2y_0 \end{aligned} \tag{B3}$$

In our particular case, H_0 is the rate matrix of the unperturbed lattice, including the isolated trap, whereas U introduces the connectivity between the two as a perturbation. There are two differences with respect to the standard perturbation approach. Firstly, the unperturbed lattice contains two independent equilibrium states, so that the eigenvalue under consideration is degenerate. Secondly, the perturbation matrix U can be asymmetric. We assume that H_0 is symmetric, and thus has an orthonormal basis of eigenvectors x_n with corresponding eigenvalues λ_n, and that the asymmetry of U does not impair diagonalization. In that case, the first equation of B3 indicates that μ_0 is an eigenvalue of H_0:

$$\mu_0 = \lambda_n \tag{B4}$$

If this eigenvalue is degenerate, y_0 is not determined but can be further investigated with the help of a projection operator on the eigenspace $P_n x = \sum_{\lambda_m} = \lambda_n(x_m, x)x_m$. From the second equation in B3 it is readily demonstrated that:

$$P_nUy_0 = \mu_1y_0 \qquad P_nU^Ty_0' = \mu_1y_0' \tag{B5}$$

From the first equality it appears that y_0 is not just an eigenvector of H_0, but also of P_nU, and μ_1 is its eigenvalue. We assume that P_nU has no degenerate eigenvalues, and thus lifts the degeneracy. In the second expression, U^T is the transposed matrix of U, whereas y'_0 is part of the expression for the adjoint eigenvector $y' = \sum y'_n\alpha^n$ of H^T, adjoint to y. This simultaneous determination of the adjoint eigenvector is necessary, because the matrix is no longer symmetric to this order. Finally, from the third equation in B3, the second order term is obtained:

$$\begin{aligned} \mu_2 &= \frac{(y_0', Uy_1) - \mu_1(y_0', y_1)}{(y_0', y_0)} = \frac{(y_0', Uy_1) - (y_0', UP_ny_1)}{(y_0', y_0)} \\ &= \sum_{\lambda_n \neq \mu_0} \frac{(x_n, y_1)(y_0', Ux_n)}{(y_0', y_0)} = \sum_{\lambda_n \neq \mu_0} \frac{(x_n, Uy_0)(y_0', Ux_n)}{(\mu_0 - \lambda_n)(y_0', y_0)} \end{aligned} \tag{B6}$$

The results above can be applied to a lattice with trap. We consider perturbation of the eigenvalues $\lambda_0 = \lambda_1 = 0$ corresponding to the equilibrium states: $x_0 = \{1, 0, \cdots, 0\}$ and $x_1 = \{0, 1, \cdots, 1\}/(N-1)$ on the trap and the lattice, respectively. Note that x_1 is not normalized. The zeroth order perturbation is $\mu_0 = 0$ for both states. To obtain μ_1, we must study P_0U. By straightforward calculation we find:

$$\begin{aligned} (x_0, Ux_0)/|x_0|^2 &= W_{00} = -\gamma - \sum_{i\neq 0} W_{i0} = -\gamma - \bar{W}_D \\ (x_1, Ux_0)/|x_1|^2 &= \sum_{i\neq 0} W_{i0} = \bar{W}_D \\ (x_0, Ux_1)/|x_0|^2 &= \frac{1}{N-1}\sum_{i\neq 0} W_{0i} = \bar{W}_T \\ (x_1, Ux_1)/|x_1|^2 &= \frac{1}{N-1}\sum_{i\neq 0} W_{ii} = -\frac{1}{N-1}\sum_{i\neq 0} W_{0i} = -\bar{W}_T \end{aligned} \tag{B7}$$

All coefficients are directly expressed in the effective transfer rates as defined in Eq. 7 in the text. From this, the matrix of P_0U can be expressed in the basis $\{x_0, x_1\}$:

$$P_0U = \begin{bmatrix} -\gamma - \bar{W}_D & \bar{W}_T \\ \bar{W}_D & -\bar{W}_T \end{bmatrix} \tag{B8}$$

This is identical to the rate matrix for a two level system, and the first order perturbations of the two eigenvalues are equal to the time constants of this system, i.e., $\mu_{1\pm} = \lambda_\pm$. The corresponding eigenvectors are $y_{0\pm} = (\bar{W}_T + \lambda_\pm)x_0 + \bar{W}_Dx_1$ (again, not normalized). The adjoint eigenvector $y'_{0\pm} = (\bar{W}_T + \lambda_\pm)x_0 + (N-1)\bar{W}_Tx_1$ is similarly obtained.

Because in general, P_0U lifts the degeneracy, the second order perturbation can be evaluated with Eq. B6. It is necessary to include the other eigenvectors x_n of H_0 and assume that the transfer only occurs between the trap and a set Ω of neighbors in the lattice at fixed rates $W_{0i} = W_T$ and $W_{i0} = W_D$. With this limitation we obtain:

$$\begin{aligned} (x_n, Ux_0) &= \sum_{i\neq 0} x_{ni}W_{i0} = \bar{W}_D \sum_{i\in\Omega} \frac{x_{ni}}{z} \\ (x_n, Ux_1) &= \sum_{i\neq 0} \frac{x_{ni}W_{ii}}{N-1} = -\bar{W}_T \sum_{i\in\Omega} \frac{x_{ni}}{z} \\ (x_0, Ux_n) &= \sum_{i\neq 0} W_{0i}x_{ni} = (N-1)\bar{W}_T \sum_{i\in\Omega} \frac{x_{ni}}{z} \\ (x_1, Ux_n) &= \sum_{i\neq 0} \frac{W_{ii}x_{ni}}{N-1} = -\bar{W}_T \sum_{i\in\Omega} \frac{x_{ni}}{z} \end{aligned} \tag{B9}$$

The presence of the x_n is limited only to the average of their entries over Ω. With $y_{0\pm}$ and $y'_{0\pm}$ obtained above this leads to:

$$(x_n, Uy_{0\pm}) = \lambda_\pm \bar{W}_D \sum_{i\in\Omega} \frac{x_{ni}}{z}$$

$$(y'_{0\pm}, Ux_n) = \lambda_\pm (N-1)\bar{W}_T \sum_{i\in\Omega} \frac{x_{ni}}{z} \qquad \text{(B10)}$$

$$(y'_{0\pm}, y_{0\pm}) = (\bar{W}_T + \lambda_\pm)^2 + \bar{W}_T\bar{W}_D$$

from which the second order perturbation is found by substitution in Eq. B6:

$$\mu_2 = \frac{\lambda_\pm^2 (N-1)\bar{W}_T\bar{W}_D}{(\bar{W}_T + \lambda_\pm)^2 + \bar{W}_T\bar{W}_D} g_d(N) W_h^{-1} \qquad \text{(B11)}$$

where:

$$g_d(N) = \sum_{\lambda_n \neq 0} \frac{W_h}{-\lambda_n} \left(\sum_{i\in\Omega} \frac{x_{ni}}{z} \right)^2 \qquad \text{(B12)}$$

is a function related only to the structure of the lattice. It is analogous to the structure function $h_d(N)$ for the local trap models, except that each term is scaled with the above-mentioned average entry of the corresponding eigenvector.

With these results, we can describe the kinetics of the perturbed two-level system by two rate constants: $\mu_\pm = \mu_{1\pm} + \mu_{2\pm} + O(W_h^{-2})$. They may also be expressed as time constants:

$$\tau_\pm(W_h^{-1}) = -\frac{1}{\mu_\pm} = -\frac{1}{\lambda_\pm} \qquad \text{(B13)}$$

$$+ \frac{(N-1)\bar{W}_T\bar{W}_D}{(\bar{W}_T + \lambda_\pm)^2 + \bar{W}_T\bar{W}_D} g_d(N) W_h^{-1} + O(W_h^{-2})$$

APPENDIX C

Averaged orientation factor for transfer to the reaction center

As modelled by Förster's theory, and illustrated in Eq. 16, the rate of exciton transfer between two pigments depends, besides other parameters, on their relative position (r_{12}) and the orientation of their transition dipole moments (μ_1 and μ_2). In the case of point dipoles, the effect of the orientations is determined by the square of the orientation factor κ for dipole-dipole interaction:

$$\kappa^2 = ((\hat{\mu}_1, \hat{\mu}_2) - 3(\hat{\mu}_1, \hat{r}_{12})(\hat{\mu}_2, \hat{r}_{12}))^2 \qquad \text{(C1)}$$

where "^" denotes the unit vectors. The orientation factor κ^2 varies between zero and four and has considerable effect on individual transfer rates. More serious, however, is that even in a symmetric structure, the average transfer to and from particular sites can be considerably affected. We illustrate this for transfer between a single RC and a symmetric ring of N LHA sites around it. The transition dipole moments of the RC and the LHA pigments are assumed to be parallel to the (xy) plane of the ring, and the RC is arbitrarily placed in the origin of the coordinate system. Its transition dipole moment is characterized by a single angle (α):

$$\hat{\mu}_{RC} = \begin{bmatrix} \cos\alpha \\ \sin\alpha \\ 0 \end{bmatrix} \qquad \text{(C2)}$$

The LHA pigments are equally spaced across the ring with angles $\theta = 2\pi/N$ between them, whereas the transition dipole moments of each pigment is at an angle (ϕ) with its position vector. Vertical displacement between the LHA ring and the RC is included by the angle (δ):

$$\hat{\mu}_n = \begin{bmatrix} \cos(n\theta + \phi) \\ \sin(n\theta + \phi) \\ 0 \end{bmatrix} \qquad \hat{r}_n = \begin{bmatrix} \cos\delta\cos(n\theta) \\ \cos\delta\sin(n\theta) \\ \sin\delta \end{bmatrix} \qquad \text{(C3)}$$

The dipole-dipole orientation factor κ_n between the RC and pigment n is readily found and the average of κ_n^2 can be obtained by considering that for any $N \neq 2$ and any angles β, β_1, and β_2, $\langle\cos(2n\theta + \beta)\rangle = 0$, so that $\langle(n\theta + \beta_1)\cos(n\theta + \beta_2)\rangle = \cos(\beta_1 - \beta_2)/2$, and thus:

$$\langle\kappa_n^2\rangle = \langle(\cos(n\theta + \phi - \alpha) - 3\cos\delta^2\cos\phi\cos(n\theta - \alpha))^2\rangle$$

$$= \frac{1 + 3\cos\delta^2(3\cos\delta^2 - 2)\cos\phi^2}{2} \qquad \text{(C4)}$$

which is independent of N and the orientation α of the RC. If the RC and the LHA pigments are in the one plane $\delta = 0$, and the result simplifies to:

$$\langle\kappa_n^2\rangle = \frac{1 + 3\cos\phi^2}{2} \qquad \text{(C5)}$$

The average orientation factor varies between 0.5 for tangential arrangement ($\phi = \pi/2$) and 2 for radial arrangement ($\phi = 0$) of the LHA pigments. This variation decreases for nonzero values of δ.

This work was financially supported by the Dutch Organization for Scientific Research (NWO), the Foundation for Life Sciences (SLW), EC contract 92–0796 and NATO contract 940851. Leonas Valkunas acknowledges support from COMPAS. The authors thank Frank van Mourik and Gert van der Zwan for their valuable discussion of the manuscript.

REFERENCES

Aagaard, J., and W. R. Sistrom. 1972. Control of synthesis of reaction center and antenna bacteriochlorophyll in photosynthetic bacteria. *Photochem. Photobiol.* 15:209–225.

Abdourakhmanov, I. A., R. V. Danielius, and A. P. Razjivin. 1989. Efficiency of excitation trapping by reaction centres of complex B890 from Chromatium minutissimum. *FEBS lett.* 245:47–50.

Bakker, J. G. C., R. van Grondelle, and W. T. F. den Hollander. 1983. Trapping, loss and annihilation of excitations in photosynthetic systems. II. Experiments with the purple bacteria *Rhodospirillum rubrum* and *Rhodopseudomonas capsulata*. *Biochim. Biophys. Acta.* 725:508–518.

Beekman, L. M. P., F. van Mourik, M. R. Jones, H. M. Visser, C. N. Hunter, and R. van Grondelle. 1994. Trapping kinetics in mutants of the photosynthetic purple bacterium *Rhodobacter sphaeroides*: influence of the charge separation rate and consequences for the rate-limiting step in the light-harvesting process. *Biochemistry.* 33:3143–3147.

Bradforth, S. E., R. Jimenez, F. van Mourik, R. van Grondelle, and G. R. Fleming. 1995. Excitation transfer in the core light harvesting complex (LH-1) of *Rhodobacter sphaeroides*: an ultrafast fluorescence depolarization and annihilation study. *J. Chem. Phys.* 99:16,179–16,191.

Cogdell, R. J., Lindsay, J. G., J. Valentine, and I. Durant. 1982. A further characterization of the B890 light-harvesting pigment protein complex from *Rhodospirillum rubrum* strain S1. *FEBS letters.* 150:151–154.

den Hollander, W. T. F., J. G. C. Bakker, and R. van Grondelle. 1983. Trapping, loss and annihilation of excitations in a photosynthetic system. I. Theoretical aspects. *Biochim. Biophys. Acta.* 725:492–507.

Dracheva, T. V., V. I. Novoderezhkin, and A. P. Razjivin. 1994. Exciton theory of spectra and energy transfer in photosynthesis: spectral hole burning in the antenna of purple bacteria. *J. Chem. Phys.* 194:223–235.

Förster, T. 1965. Delocalized excitation and excitation transfer. *In* Modern Quantum Chemistry. III. Action of light and organic crystals. O. Sinanoglu, editor. Academic Press, New York. 93–137.

Freiberg, A., V. I. Godik, T. Pullerits, and K. Timpmann. 1989. Picosecond dynamics of directed excitation transfer in spectrally heterogeneous light-harvesting antenna of purple bacteria. *Biochim. Biophys. Acta.* 973:93–104.

Hemenger, R. P., R. M. Pearlstein, and K. Lakatos-Lindenberg. 1972. Incoherent exciton quenching on lattices. *J. Math. Phys.* 13:1056–1063.

Karrasch, S., P. A. Bullough, and R. Ghosh. 1995. The 8.5 Å projection map of the light-harvesting complex I from Rhodospirillum rubrum reveals a ring composed of 16 subunits. *EMBO J.* 14:631–638.

Knox, R. S. 1968. On the theory of trapping of excitation in the photosynthetic unit. *J. Theor. Biol.* 21:244–259.

Kudzmauskas, S. P., L. L. Valkunas, and A. Y. Borisov. 1983. A theory of excitation transfer in photosynthetic units. *J. Theor. Biol.* 105:13–23.

Loach, P. A., P. S. Parkes, J. F. Miller, S. B. Hinchigeri, and P. M. Callahan. 1985. Structure function relationships of the bacteriochlorophyll protein-light-harvesting complex of *Rhodospirillum rubrum*. *In* Cold Spring Harbor Symposium on Molecular Biology of the Photosynthetic Apparatus. C. Arntzen, L. Bogorad, S. Bonitz, and K. Steinback, editors. Cold Spring Harbor, New Jersey. 197–209.

Martin, J. L., J. Breton, A. J. Hoff, A. Migus, and A. Antonetti. 1986. Femtosecond spectroscopy of electron transfer in the reaction center of the photosynthetic bacterium *Rhodopseudomonas sphaeroides* R-26: direct electron transfer from the dimeric bacteriochlorophyll primary donor to the bacteriopheophytin acceptor with a time constant of 2.8 ± 0.2 psec. *Proc. Nat. Acad. Sci. USA.* 83:957–961.

McDermott, G., S. M. Prince, A. A. Freer, A. M. Hawthornthwaite-Lawless, M. Z. Papiz, R. J. Cogdell, and N. W. Isaacs. 1995. Crystal structure of an integral membrane light-harvesting complex from photosynthetic bacteria. *Nature.* 374:517–521.

Meckenstock, R. U., R. A. Brunisholz, and H. Zuber. 1992. The light-harvesting core-complex and the B820-subunit from *Rhodospirillum marina*. Part I: The purification and characterization. *FEBS lett.* 311:128–134.

Monger, T. G. and W. W. Parson. 1970. Singlet-triplet fusion in *Rhodopseudomonas sphaeroides* chromatophores. A probe of the organization of the photosynthetic apparatus. *Biochim. Biophys. Acta.* 460:393–407.

Otte, S. C. M., F. A. M. Kleinherenbrink, and J. Amesz. 1993. Energy transfer between the reaction center and the antenna in purple bacteria. *Biochim. Biophys. Acta.* 1143:84–90.

Pearlstein, R. M. 1982. Excitation migration and trapping in photosynthesis. *Photochem. Photobiol.* 35:835–844.

Pearlstein, R. M. 1992. Kinetics of exciton trapping by monocoordinate reaction centers. *J. Lumin.* 51:139–147.

Pullerits, T., and A. Freiberg. 1992. Kinetic model of primary energy transfer and trapping in photosynthetic membranes. *Biophys. J.* 63:879–896.

Pullerits, T., K. J. Visscher, S. Hess, V. Sundström, A. Freiberg, K. Timpmann, and R. van Grondelle. 1994. Energy transfer in the homogeneously broadened core antenna of purple bacteria: a simultaneous fit of low-intensity picosecond absorption and fluorescence kinetics. *Biophys. J.* 66:236–248.

Schmidt, S., T. Arlt, P. Hamm, C. Lauterwasser, U. Finkele, G. Drews, and W. Zinth. 1993. Time-resolved spectroscopy of the primary photosynthetic process of membrane-bound reaction centers from an antenna deficient mutant of *Rhodobacter capsulatus*. *Biochim. Biophys. Acta.* 1144:385–390.

Somsen, O. J. G., F. van Mourik, R. van Grondelle, and L. Valkunas. 1994. Energy migration and trapping in a spectrally and spatially inhomogeneous light-harvesting antenna. *Biophys. J.* 66:1580–1596. Erratum: *Biophys. J.* 67:484.

Stark, W., W. Kühlbrandt, I. Wildhaber, E. Wehrli, and K. Mühlethaler. 1983. The structure of the photoreceptor unit of *Rhodopseudomonas viridis*. *EMBO J.* 3:777–783.

Timpmann, K., A. Freiberg, and V. I. Godik. 1991. Picosecond kinetics of light excitations in photosynthetic purple bacteria in the temperature range 300–4K. *Chem. Phys. Lett.* 182:617–622.

Timpmann, K., F. G. Zhang, A. Freiberg, and V. Sundström. 1993. Detrapping of excitation energy from the reaction centre in the photosynthetic purple bacterium *Rhodospirillum rubrum*. *Biochim. Biophys. Acta.* 1183:185–193.

Timpmann, K., A. Freiberg, and V. Sundström. 1995. Energy trapping and detrapping in the photosynthetic bacterium rhodopseudomonas viridis: transfer-to-trap-limited dynamics. *J. Chem. Phys.* 194:275–583.

Trinkunas, G., and L. Valkunas. 1989. Exciton-exciton annihilation in picosecond spectroscopy of molecular systems. *Exp. Tech. Physik.* 37: 455–458.

Valkunas, L. L., S. P. Kudzmauskas, and V. Y. Liuolia. 1986. Noncoherent migration of excitation in impure molecular structures. *Lit. Fiz. Sbornik.* 26:3–15.

Valkunas, L. 1989a. Nonlinear processes in picosecond spectroscopy of photosynthetic systems. *In* Proceedings of the 5th School on Quantum Electronics. Lasers - Physics and Applications. (ed. AY Spasov). World Scientific Co., Singapore 541–560.

Valkunas, L. 1989b. Energy migration in antenna systems. In: Proceedings of the VIth International Conference on Energy and Electron Transfer. (eds. J Fiala and J Pokorny). Charles University Prague. pp 87–91.

Valkunas, L., F. van Mourik, and R. van Grondelle. 1992. On the role of spectral and spatial antenna inhomogeneity in the process of excitation energy trapping in photosynthesis. *Photochem. Photobiol.* 15:159–170.

Valkunas, L., O. I. G. Somsen, F. van Mourik, and R. van Grondelle. 1994. Energy migration in spectrally inhomogeneous photosynthetic antenna systems. *Lithuanian Journal of Physics.* 34:89–93.

Valkunas, L., G. Trinkunas, V. Liuolia, and R. van Grondelle. 1995. Nonlinear annihilation of excitations in photosynthetic systems. *Biophys. J.* 69:1117–1129.

van Grondelle, R., H. Bergström, V. Sundström, and T. Gillbro. 1987. Energy transfer within the bacteriochlorophyll antenna of purple bacteria at 77K, studied by picosecond absorption recovery. *Biochim. Biophys. Acta.* 894:313–326.

van Grondelle R., J. P. Dekker, T. Gillbro, and V. Sundström. 1994. Energy transfer and trapping in photosynthesis. *Biochim. Biophys. Acta.* 1187:1–65.

van Mourik, F., J. R. van der Oord, K. J. Visscher, P. S. Parkes-Loach, P. A. Loach, R. W. Visschers, and R. van Grondelle. 1991. Exciton interaction in the light-harvesting antenna of photosynthetic bacteria studied with triplet-singlet spectroscopy and singlet-triplet annihilation on the B820 subunit form of *Rhodospirillum rubrum*. *Biochim. Biophys. Acta.* 1059:111–119.

Visschers, R. W., M. C. Chang, F. van Mourik, P. S. Parkes-Loach, B. A. Heller, P. A. Loach, and R. van Grondelle. 1991. Fluorescence polarization and low-temperature absorption spectroscopy of a subunit form of light-harvesting complex I from photosynthetic purple bacteria. *Biochemistry.* 30:5734–5742.

Visser, H. M., O. J. G. Somsen, F. van Mourik, S. Lin, I. H. M. van Stokkum, and R. van Grondelle. 1995. Direct observation of sub-picosecond equilibration of excitation energy in the light harvesting antenna of *Rhodospirillum rubrum*. *Biophys. J.* 69:1083–1099.

Vredenberg, W. J., and L. N. M. Duysens. 1963. Transfer of energy from bacteriochlorophyll to a reaction centre during bacterial photosynthesis. *Nature.* 197:355–357.

Xiao, W., S. Lin, A. K. W. Taguchi, and N. W. Woodbury. 1994. Femtosecond pump-probe analysis of energy and electron transfer in photosynthetic membranes of *Rhodobacter capsulatus*. *Biochemistry.* 33:8313–8322.

Zuber, H., and R. A. Brunisholz. 1991. Structure and function of antenna polypeptides and chlorophyll-protein complexes: principles and variability. In Chlorophylls. H. Scheer, editor. CRC Press, Boston. 627–719.